Proceedings of International Conference on Heat Exchanger Fouling and Cleaning - 2015 (Peer-reviewed)
June 07 - 12, 2015, Enfield (Dublin), Ireland
Editors: M.R. Malayeri, H. Müller-Steinhagen and A.P. Watkinson
Published online
www.heatexchanger-fouling.com

DEPOSITION FROM A SOUR HEAVY OIL UNDER INCIPIENT COKING CONDITIONS: WALL SHEAR STRESS EFFECTS AND MECHANISM

W. Wang and A.P. Watkinson[1]

[1] Department of Chemical & Biological Engineering, The University of British Columbia
2360 East Mall, Vancouver, BC V6T 1Z3 Canada
apw@chbe.ubc.ca

ABSTRACT

In vacuum tower furnaces, heavy and sour feedstocks at elevated temperatures promote fouling due to both corrosion product formation and carbonaceous species deposition, which has been studied in a batch isothermal unit with an atmospheric tower bottoms (ATB) sample which contains 4.1wt%. sulphur and 744wppm dissolved iron. Previously, the effects of temperature on several types of metal surfaces were reported at fixed rotational speed. In this paper, the effects of wall shear stress (maximum 13.7 Pa), and additions of iron and sulphur species are investigated at two typical bulk temperatures over 24 hour periods on carbon steel surfaces. Results indicate that a transitional shear stress region was observed for 390°C. Thioether added to the oil contributed significantly to deposition at 380°C. Addition of particulate Fe_2O_3 did not markedly promote deposit build-up. The probable fouling mechanism is discussed according to the results of the prior and current work.

INTRODUCTION

Fouling of furnaces negatively affects profitability of refinery operations. Typical vacuum tower furnace outlet temperatures are in the range 390°C to 450°C. ATB is a highly viscous and polar heavy oil fraction, which has a strong tendency to convert to coke under furnace operating conditions.

Sulphidic corrosion is widely observed in oil processing especially above temperatures of 260°C. In sour oils, concentrated sulphur compounds will react with iron in the oil or on the internal surface of the furnace tubes to generate iron sulphide. Thus iron sulphide has been a key component of foulants in heat exchangers and furnaces, as suggested by Wiehe (2008). Carbonaceous species also deposit from oils, leading to a complex mechanism of fouling. Stephenson et al. (2011) have studied corrosion of 316 stainless and pure iron wires in atmospheric bottoms fraction of a crude oil.

In previous work (Wang and Watkinson, 2015), an isothermal rotary cylinder device was used to investigate the effect of bulk temperature from 380-410°C on deposit formation in a 24-hour period on rings of carbon steel (CS), 9-chrome (9-Cr), 317 Stainless steel (SS317), Incoloy 825 and chrome-plated carbon steel (Cr-CS). Deposits were characterized by their % carbonaceous and % ash contents, which are related to the two mechanisms involved - coke formation and corrosion to form metal sulphides. At low temperature (380°C), the deposits on CS and 9-Cr were about 70-80% ash, giving evidence of the role of corrosion, whereas for the non-corroding surfaces, deposits were over 90% carbonaceous material. At higher temperatures, as coking became more important, the ash fraction of deposits on the corroding surfaces (CS and 9-Cr) decreased. Radial deposit profiles of iron, carbon and sulphur from the metal surface outwards to about 20 microns, indicated most iron in the deposit came from the metal surface rather than the bulk oil.

Flow past a surface is widely known to affect the build-up of fouling layers. At fixed temperature, fouling rates may be correlated by a flow parameter such as bulk velocity, flow Reynolds number or wall shear stress. Much literature shows that fouling rates of oils decrease with increasing flow velocity (Crittenden, 1988; Watkinson, 2007; Krueger and Pouponnot, 2009; Watkinson and Li, 2009). Effects of flow are captured in models of the fouling process, such as that of Epstein (1994), where the deposition process is viewed as mass transport of foulants in series with an n-th order chemical reaction attachment step. In this model, the rate of fouling goes through a maximum with increasing flow parameter, as transport increases with velocity, and attachment is inversely proportional to wall shear stress. Joshi (2009) found that in crude oil pre-heat trains, fouling rate varied as $(\tau_w)^{-1.63}$.

Corrosion rates are also reported to increase with velocity, or wall shear stress (Silverman, 2004) and knowledge of wall shear stress is required to make corrosion rate measurements meaningful.

Exact shear effect of fluid on the fouling buildup rate or composition of foulant is still not understood very well (Stephenson et al., 2011).

The impact of bulk fluid temperature, and metal composition on deposition has been discussed in our previous study (Wang and Watkinson, 2015), and two different regimes identified according to the dominant deposit composition. Corrosion controlled or incipient coking regimes are proposed to describe the remarkable difference of fouling rates and deposit compositions on corroding surfaces at lower (<380°C) and higher (>390°C) bulk temperatures. For non-corroding surfaces, only the latter regime occurred at temperatures tested. In this work,

the effects of rotational speed on the build-up of deposits were therefore investigated, in order to arrive at a working mechanism for deposition in this system.

EXPERIMENTAL

Isothermal fouling experiments were performed in a 600 ml Parr instrument Model 4563 batch reactor which contained a rotating cylinder (Fig. 1). The detailed description of the experimental set-up and operation procedure are seen in our former paper (Wang and Watkinson, 2015). Carbon steel rings were fixed to a machinable ceramic cylinder which was rotated in the range of 150-1 500rpm. Rotational speed was determined with a REED AT-6 tachometer.

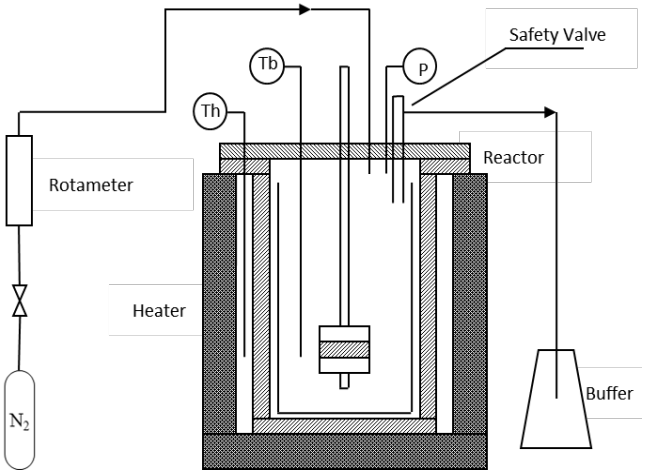

Fig. 1 Schematic diagram of stirred rotating cylinder batch reactor.

Test oil was an atmospheric tower bottom (ATB) oil sample provided by Syncrude Canada Ltd. The physical and chemical properties of the ATB oil have been discussed in our former paper (Wang and Watkinson, 2015). Type 1018 low carbon steel rings were used. In order to maintain a consistent surface roughness in all experiments, rings were polished using the same procedure (Wang and Watkinson, 2015), and the roughness has been successfully controlled in the range of 0.31-0.36μm.

Two typical bulk temperatures were selected to compare shear stress effects under conditions where deposits contained mainly ash, or mainly carbonaceous material. The experiment duration was set to 24 hours after heat-up procedures. Rate of film growth has been shown to be roughly constant over this period. Deposit rate is expressed as mm/year, in order to compare with corrosion studies. Rotating speeds in the experiments were 150-1 200rpm.

After each experiment, the thickness of deposit was calculated from a photographic method (Wang and Watkinson, 2015).

Since small and large pieces of deposit would fall of the ring surfaces to the oil during the experiment, and this kind of problem frequently crops up, a special method was used to calculate the area of deposit debris in MATLAB. Then by measuring the weight of each piece, the density of deposit as well as the total deposition weight can be calculated.

The deposit was characterized with Thermogravimetric Analysis (TGA) (Coletti and Hewitt), which yields a measure of volatiles, fixed carbon and ash. The carbonaceous content of the deposit was given by the sum of volatiles and fixed carbon. Volatiles represent the oil fraction with boiling point from low to high. Fixed carbon represents the coke. Ash content reflects the metal in the deposit from either metallic contaminants in the oil, or from corrosion of the metal surface.

In order to study the transfer of metal during the experiment, we measured the concentration of metal elements in ATB, bulk coke, ring surface deposit and spent oil, respectively, by Inductively Coupled Plasma (ICP) (Kishore Nadkarni), and did mass balances for the most abundant elements in ATB. To determine the crystal structure of Fe compounds in the oil and deposit, X-ray Diffraction (Coletti and Hewitt) was adopted for deposits from both spent oil and ring surfaces.

SULPHIDIC CORROSION IN HEAVY OIL

Most sulphur species in heavy oil are thiophene derivatives (70-80%) and other thioether (20-30%) (Waldo et al., 1991; Mullins et al., 2007; Javadli and de Klerk, 2012). More than half of thiophene is with 5+ rings. Other sulphur species are negligible. Thiophene derivatives are so stable at high temperatures that they can only decompose to small derivatives (Groysman, 2014). Thiophene cores are very difficult to destroy to release active sulphur (H_2S) without catalysts.

Although thioether is stable, it is still able to decompose to thiol, H_2S, alkene and thiophene (Nikonov and Senning, 1989). Then thiol rapidly decomposes to H_2S and alkene. Therefore, the H_2S in our oil is very likely to come from thioether. H_2S will decompose to generate element sulphur at high temperatures, which is highly active and may readily react with Fe.

SHEAR STRESS IN ANNULAR FLOW SYSTEM

For the present geometry, the wall shear stress can be calculated from the rotational speed as (Silverman, 1984; Efird et al., 1993):

$$\tau_w = 0.079\,\mathrm{Re}^{-0.3}\,\rho u_{cyl}^2 \qquad (1)$$

in which $\mathrm{Re} = \dfrac{d_{cyl} u_{cyl} \rho}{\mu}$, and $u_{cyl} = \dfrac{\pi d_{cyl} F}{60}$.

For rotation speeds of 150-1 200rpm, the range of shear stress on ring surfaces is 0.4-13.7Pa, and Reynolds number is 7 000-56 000.

SHEAR STRESS EFFECTS UNDER TWO REGIMES

Isothermal fouling experiments were run with carbon steel rings and Syncrude ATB at lower (380°C) and higher (390°C) bulk temperature, pressure is 2.4MPa (350psig), at different rotational speeds (150-1 200rpm) for 24 hours. After each run, deposit thickness was determined. Fouling rate and deposit density at different wall shear stress under

both corrosion controlled regime and incipient coking regime are seen in Fig. 2-3.

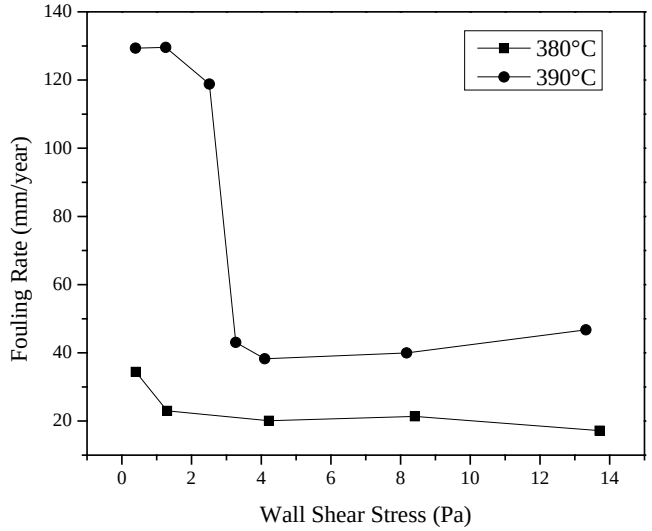

Fig. 2 Fouling rate under two temperature regimes versus wall shear stress.

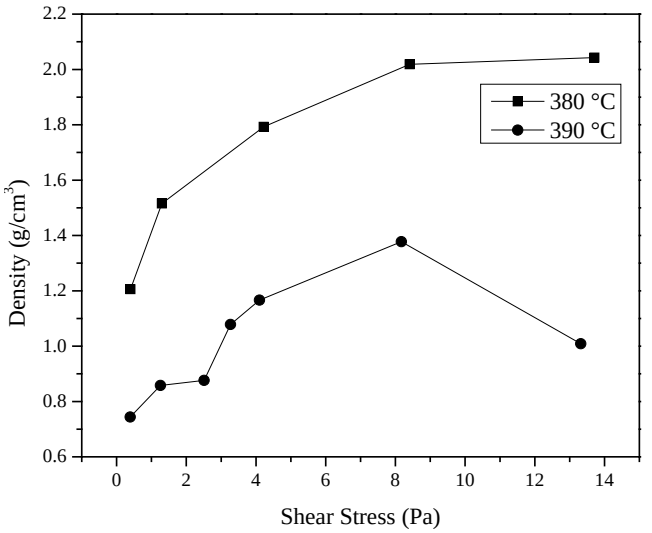

Fig. 3 Deposit density under two temperature regimes versus wall shear stress.

As shown in Fig. 2, fouling rate is 10-30 mm/year and 40-130mm/year for 380°C and 390°C runs, respectively. A sudden change of thickness for shear stress of 1-3Pa for 390°C runs was observed. Deposit rate is very sensitive to wall shear stress in this range.

Fig. 3 indicates deposit density increases with shear stress at both temperatures, i.e. at a given temperature, higher shear stress made the deposit more compact. For the 390°C experiments, deposit density is 0.7-1.4g/cm^3 which is close to 0.7-1.1g/cm^3 reported for petroleum coke by Edwards et al. (2011)For 380°C, the deposit density (1.2-2.1g/cm^3) , is higher than at 390°C as the deposit contains more FeS, which has a density of 4.8g/cm^3.

As mentioned above, TGA was adopted to determine the weight of carbonaceous matter and ash in the depsosits. Results are seen in Fig. 4-5. At 380°C (Fig. 4), the mass of ash is about 5 times the mass of carbonaceous material in the deposit, and both components are independent of the wall shear stress.

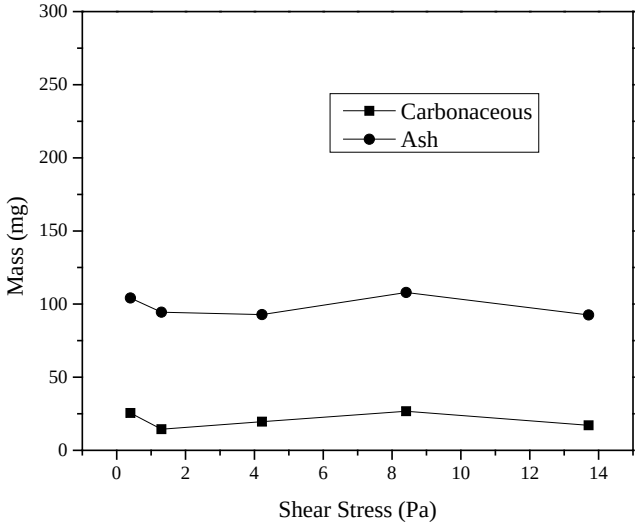

Fig. 4 Mass of carbonaceous matter and ash for corrosion controlled regime (380°C).

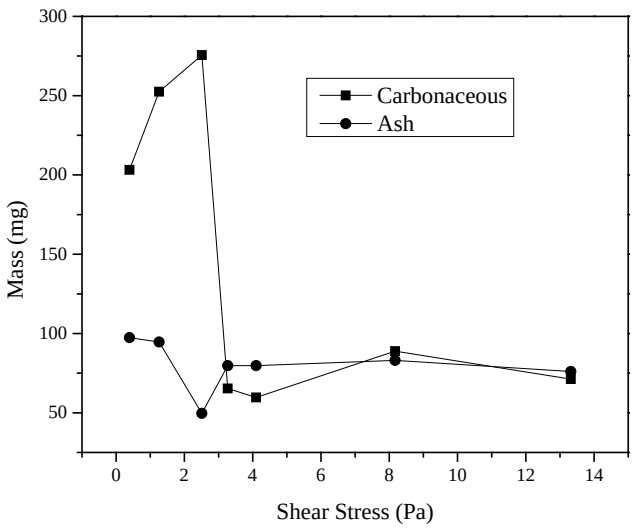

Fig. 5 Mass of carbonaceous matter and ash in deposits for incipient coking regime (390°C).

With increasing shear stress, the proportions of carbonaceous matter and ash (Fig. 4) are fairly constant at 380°C. At 390°C (Fig. 5), a transitional shear stress region (0-3Pa) was found, in which deposit composition changed markedly, from being predominantly carbonaceous to a uniform ash-carbonaceous content at higher shear stresses.

Fouling with iron sulphide formation includes two processes: corrosion of the metal and coking on ring surfaces. These two types of reaction were analyzed respectively for a better understanding of the entire fouling mechanism. First the corrosion process is considered. Sulphidic corrosion in the absence of carbonaceous fouling will lead to the growth of an iron sulphide film. The coking process will be discussed in the next section.

CORROSION REACTION ANALYSIS

Corrosion due to active sulphur and naphthenic acid in oil fraction has been widely discussed (Mrowec et al., 1969; Jong et al., 2007; Bota, 2010). Naphthenic acid corrosion starts at about 216°C, and reaches a maximum in the range of 260-288°C (Zetlmeisl, 1996). At higher temperatures, thermal decomposition of naphthenic acid has been observed (Slavcheva et al., 1999; Qu et al., 2006). The onset of corrosion due to active sulphur species is at 260°C (Zetlmeisl, 1996) and corrosion rate increases at higher temperatures. Modified McConomy curves (Garverick, 1994, Lai, 2007; Albright, 2008; Javaherdashti et al., 2013), as seen in Fig. 6, show sulphide corrosion rates versus temperature on the basis of industrial experience. Modified McConomy curves are widely used to predict the corrosion rate at different operating temperatures when hydrogen is absent or less than 345kPa.

According to the curves, the corrosion rate of carbon steel is around 8.6 times that of 9Cr and 27 times of that of 18/8 stainless steel, indicating a significant change of corrosion rate when chromium content is increased from 9% to 18%. In our previous work, sudden changes were observed when chromium content in metals was 15-20%, which met the results from the curves fairly well.

Corrosion rates of carbon steel at 380°C and 390°C when sulphur content is 0.6 wt%, (Fig. 6) are expected to be 1.48 and 1.65mm/year, respectively. Since the sulphur content in Syncrude ATB is 4.1 wt%, the corrosion rate multiplier is around 2.0. Thus in the absence of coking, the expected corrosion rates in the present work are 2.96 and 3.30mm/year, respectively, and increases by 11.5% from 380°C to 390°C. By comparison, the average measured corrosion rates for different shear stresses are 2.72 and 2.35mm/year, respectively, calculated from Fig. 4 and 5. The measured corrosion rate decreases by 13.6% from 380°C to 390°C.

The modified McConomy curves can be expressed as

$$r_1 = k_1 c_1^n = A_1 c_1^n \exp\left(-\frac{E_{a1}}{RT}\right) \quad (2)$$

Where the lumped constant A_1 contains an alloy factor to account for the corrosion rate of different alloys and c_1^n is proportional to the corrosion rate multiplier as shown in Fig. 6, with n~ 0.37.

The temperature dependence can be expressed via Arrhenius form as:

$$\ln(r_1) = \ln\left(A_1 c_1^n\right) - \frac{E_{a1}}{R}\left(\frac{1}{T}\right) \quad (3)$$

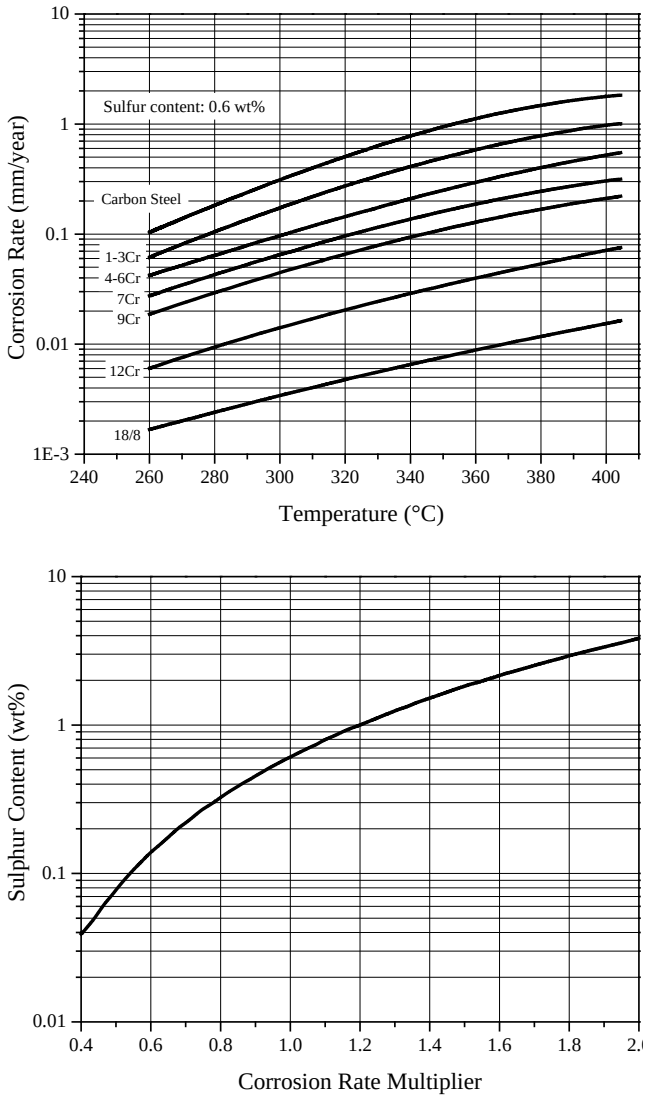

Fig. 6 Modified McConomy Curves and corrosion rate multiplier.

With assumed constant c_1, activation energy E_{a1} can be obtained by plotting $\ln(r_1)$ with (1/T) in the range of 380-390°C, as shown in Fig. 7, where the activation energy is calculated as 32.1kJ/mol.

The same calculation procedure was used to determine the activation energy in the same range of temperature for the rate of corrosion (measured by ash content) in this work, as shown in Fig. 8. For experiments in the temperature range of 380-400°C and at 300rpm, as the temperature increased, the growth rate decreased, corresponding to an activation energy of corrosion is -99.2kJ/mol.

Therefore, when fouling accumulates on the surface, the temperature affects the film growth rate in the opposite direction compared to the circumstance when there is no fouling on the surface.

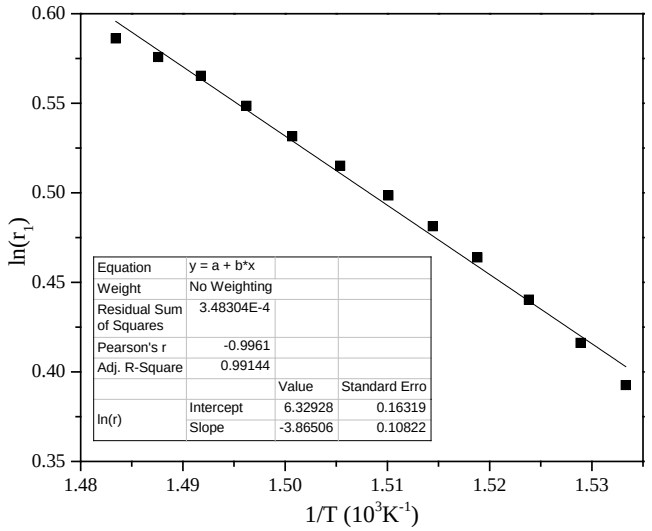

Fig. 7 Arrhenius-type plot for McConomy curves (380-400°C).

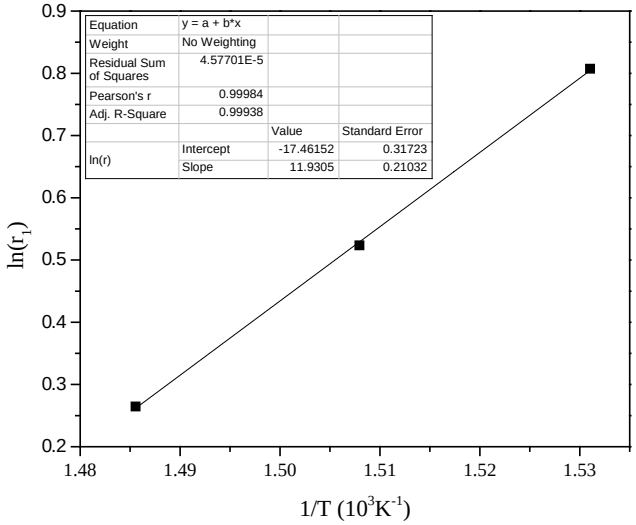

Fig. 8 Arrhenius-type plot for corrosion rate (mm/year) for experiments at 380-400°C and at 300rpm

COKING REACTION ANALYSIS

Coking reaction has been proved to be first order in the concentration of asphaltenes (Wiehe, 2008). This reaction occurs both in the bulk oil and on the ring surfaces. Activation energies were calculated for each process in the temperature range of 380-400°C. For coking in bulk oil, the decreasing concentration of asphaltene in the oil for different durations was measured to calculate rate constant k as:

$$\ln(c) = \ln(c_0) - kt \qquad (4)$$

In Equation 4, the rate constant k can be obtained by plotting ln(c) with t (second), as shown in Table 1. Then the activation energy for the bulk asphaltene disappearance can be obtained by Arrhenius plot as 342 kJ/mol.

Table 1. Rate Constant Calculation for Different Bulk Temperatures.

Bulk T, °C	Asphaltene concentration, wt%.			k, $10^6 s^{-1}$
	6 hours	12 hours	24 hours	
380	9.7	9.3	8.6	1.85
390	9.1	8.3	6.7	4.76
400	7.9	5.9	3.6	12.0

The rate of deposit mass accumulation for coke on the surface is given by dm_{fc}/dt, and was determined thermo-gravimetrically from the mass of fixed carbon in the deposit, after 24 hours. Its temperature dependence follows an Arrhenius plot (Fig. 9), from which an activation energy of 394kJ/mol was calculated. The coke deposition process appears to have a stronger temperature dependence than does the asphaltene disappearance reaction.

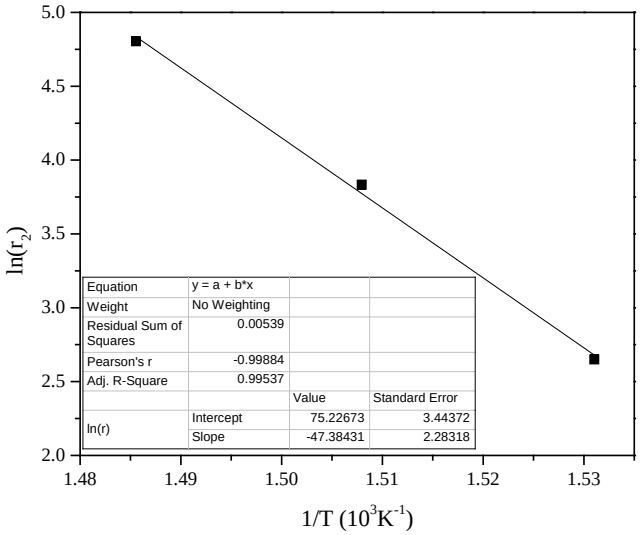

Fig. 9 Arrhenius-type plot for coke deposit rate (mg/day) for experiments at 380-400°C and at 600rpm

TRACE ELEMENTS TRANSFER IN EXPERIMENTS

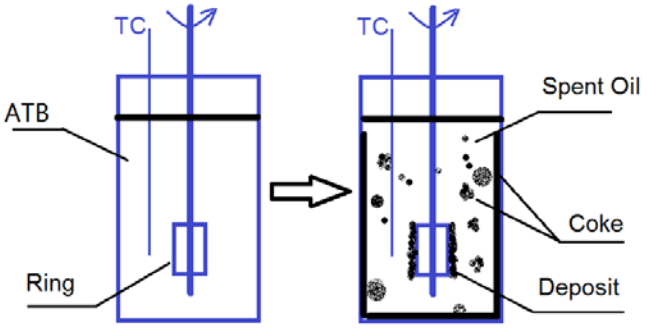

Fig. 10 Fouling products after 24-hour experiments.

Knowing how trace elements transfer between ATB, metal surfaces and other products will facilitate the understanding of fouling mechanisms. Products after each run are divided to 4 parts, including deposit, spent oil, bulk coke and gas, as shown in Fig. 10. Deposit is the foulant attached to metal surfaces. Spent oil is the liquid oil in the reactor after runs. Bulk coke is the coke floating in spent oil

and that attached to the liner wall. Gas is vapor products released from the system.

We assume the vapor is light hydrocarbon and H_2S and the trace elements only exist in deposit, spent oil and bulk coke. Compared to deposit and gas, the exact amount of bulk coke and spent oil are more difficult to determine since they are always mixed together. Therefore, we used a very fine plastic mesh to separate part of the spent oil from bulk coke, and also collected bulk coke floating in spent oil as well as that sticking to liner wall. The bulk coke was washed with toluene to remove attached spent oil and dried at 120°C for 24 hours. ICP tests were carried out for ATB and collected spent oil, bulk coke and deposit. Five most abundant inorganic elements in ATB were chosen for a mass balance. Then the average weight of spent oil and bulk coke could be determined. The results are listed in Table 2-4. All data are based on experiments with 300g ATB.

Table 2. ICP Analysis for Carbon Steel Runs at 380°C.

Element		Si	Fe	Al	V	Ni
weight (mg)	ATB	232.5	223.2	197.4	42.6	21.9
	coke	226.2	155.0	186.4	18.9	12.6
	Spent oil	0	11.1	6.8	24.8	9.3
	deposit	0	56.2	0	0.07	0.01
concentration (wppm)	ATB	775	744	658	142	73
	coke	10 800	7 400	8 900	900	600
	Spent oil	0	44	27	98	37
	deposit	0	512 400	0	600	100

Table 3. ICP Analysis for Carbon Steel Runs at 390°C.

Element		Si	Fe	Al	V	Ni
weight (mg)	ATB	232.5	223.2	197.4	42.6	21.9
	coke	206.6	161.5	232.9	22.5	15.0
	Spent oil	0	7.3	2.7	19.2	6.9
	deposit	0	53.2	0	0.21	0.03
concentration (wppm)	ATB	775	744	658	142	73
	coke	5 500	4 300	6 200	600	400
	Spent oil	0	32	12	84	30
	deposit	0	153 000	0	600	100

Si and Al arise mainly from clay in ATB from the mining process used by Syncrude. For both bulk temperature experiments (Tables 2 and 3), nearly all Si and Al are concentrated in bulk coke after runs.

Most Fe transfers from the ATB to the bulk coke, while a very small part remains in spent oil. Since the carbon steel ring surfaces are also important iron sources, it's interesting to determine the source of the iron in the spent oil, bulk coke and deposit. Thus by electroplating we coated the rings with a chromium layer which is 0.127mm in thickness, and made certain the roughness of the surface is the equal to that of carbon steel ring. Results indicated chromium is below the detection limit in either spent oil or bulk coke. No chromium is observed even in the deposit. This means that chromium is an excellent isolator which ensures no iron in spent oil, bulk coke and deposit are derived from the ring surface. Results showed only 2 000wppm Fe was found in the deposit of chrome plated carbon steel rings. This is a considerably (factor of 76) lower concentration compared to the concentration of iron in the deposit on carbons steel rings. This suggests that nearly all iron in the deposit comes from the metal surface rather than ATB. In addition, weight of iron in deposit of carbon steel for 380°C and 390°C, around 60mg, are very close to each other. This also fits the result in Fig. 5. V and Ni mainly exist in resin and asphaltene. Most of these elements transferred to coke and a small part remained in spent oil.

Table 4. ICP Analysis for Chrome Plated Carbon Steel Runs at 390°C.

Element		Si	Fe	Al	V	Ni
weight (mg)	ATB	232.5	223.2	197.4	42.6	21.9
	coke	219.2	223.0	207.9	26.5	15.1
	Spent oil	0	5.8	2.1	15.0	7.1
	deposit	0	0.15	0	0.04	0.01
concentration (wppm)	ATB	775	744	658	142	73
	coke	5 800	5 900	5 500	700	400
	Spent oil	0	27	10	70	33
	deposit	0	2 000	0	600	100

ADDITION OF IRON PARTICULATES

Table 5 Effects of Addition of Iron Oxide Particulates

Bulk Temperature	380°C	390°C
Deposit Thickness without adding Iron Particles	55.0μm	104.9μm
Deposit Thickness with addition of Iron Particles	66.4μm	90.2μm
Growth Rate Change	+21%	-14%

In order to study the fouling performance with suspended particulates in the oil, 0.316g Fe_2O_3 particles (<5 μm) was added to 300ml ATB, to give 744ppm suspended particulate. Experiments were carried out for 24 hours at bulk temperature of 380 and 390°C, with the rotating speed of 600rpm and 350psig. Results listed in Table 5 showed no significant change in deposit growth rate.

ADDITION OF ORGANIC SULPHUR

Experiments were carried out with 7.2ml dimethyl sulphide added to 300ml oil to double the organic sulphur

content in ATB, at the bulk temperatures of 380 and 390°C, and600 rpm at 350psig. Table 6 shows the change of deposit thickness with additional organic sulphur species. Increasing sulphur content resulted in increased deposit thickness in both experiments.

According to the modified McConomy Curves, the corrosion rate multiplier in this case is around 2.6, indicating the corrosion rate (FeS formation rate) is 30% higher than the value when sulphur content is 4.1wt%. For comparison, the deposit growth rate increase in Table 6 was 51% and 12% for 380 and 390°C, respectively.

Table 6 Effects of Additional Dimethyl Sulphide

Bulk Temperature	380°C	390°C
Deposit Thickness without additional dimethyl sulphide	55.0μm	104.9μm
Deposit Thickness with additional dimethyl sulphide	82.8μm	117.6μm
Growth Rate Increase	51%	12%

FOULING ROUTE WITH IRON SULPHIDE AND COKE

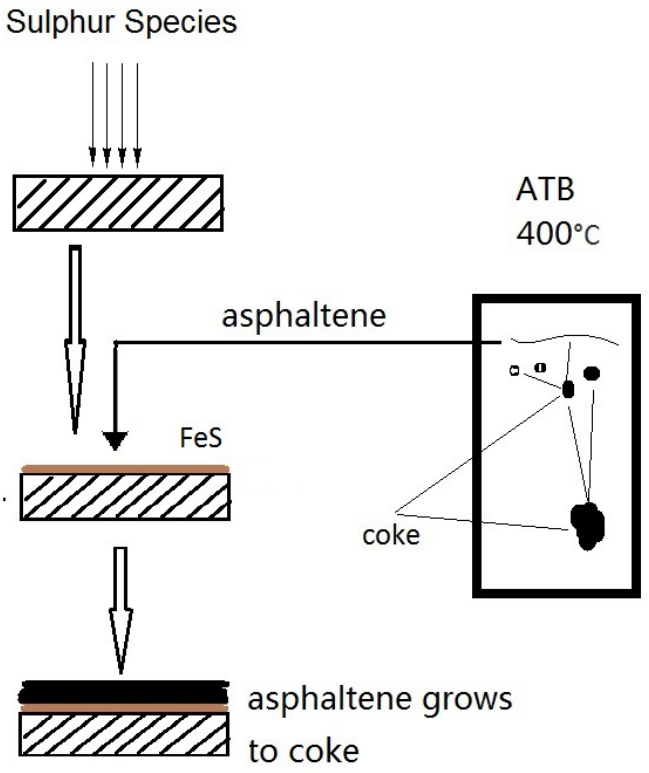

Fig. 11 Probable Fouling Mechanism under Incipient Coking Conditions.

According to our research, fouling under incipient coking conditions with iron sulphide and coke can be illustrated as Fig. 11 (based on Wiehe 2008). At temperatures higher than 380°C, Sulphur-containing species such as thioether will decompose and release H_2S and thiol, which will also generate H_2S at high temperatures. Then H_2S reacts with the metal surface to form thin FeS layer. Asphaltene or coke precursors in ATB will attach to the FeS layer, and forms coke on it. Within 2.5-5μm of the metal surface, deposits were shown to contain about 35% carbon (Wang and Watkinson, 2015). Additional organic sulphur increased fouling rate while additional iron particulates did not have a significant effect. Meanwhile, asphaltene or coke precursors will also aggregate in the bulk oil to form coke, though the coke formed in the bulk oil is not likely to accumulate on the metal surface. Coke formed directly on the metal surface will slow down the corrosion, as suggested by the negative activation energy of corrosion in our research. Most Fe in the deposit arises from the metal surface rather than bulk oil. Chromium will not transfer from metal surface to deposit or bulk oil. Coking reactions in the bulk collect most inorganic elements to the coke. Shear stress does not affect the corrosion rate significantly, but it does influence the accumulation of asphaltene or coke precursors in a small shear stress range, thus change the coking rate on metal surface. Larger shear stress makes the deposit layer more compact.

CONCLUSIONS

1. For carbon steel, the effect of shear stress on deposition is significantly different for corrosion controlled conditions (380°C) and incipient coking conditions (390°C). At 380°C, the deposition rate and composition of deposit is not largely affected by shear stress. At 390°C, there is a transitional region at lower shear stress in which fouling rate and composition of deposit (mostly carbonaceous matter) is very sensitive to shear stress.
2. In the presence of coke deposition, the corrosion rate (measured by ash content) decreases with temperature, whereas in the absence of coke deposition corrosion increases with temperature.
3. The coking process on the metal surface has higher activation energy than the bulk oil coking process. This suggests that at higher temperature, the coking reaction tends to occur preferentially on the metal surfaces.
4. Almost all the iron in the deposit comes from metal surfaces rather than from the ATB. Most iron in the ATB is consumed during the forming of bulk coke while a small part remains in the spent oil.
5. It is likely that the bulk coke formation is induced by insoluble clay particles in the ATB. Vanadium and Nickel also transfer from ATB to coke during this process.

NOMENCLATURE

A_1	lumped pre-exponential factor for corrosion of carbon steel in Modified McConomy curves, $mol^{1-n} \cdot L^{n-1} \cdot s^{-1}$
c	asphaltene concentration in oil, g/L
c_0	asphaltene concentration in feedstock oil, mol/L
c_1	oil sulphur concentration in Modified McConomy curves, mol/L
d_{cyl}	diameter of cylinder, m

E_{a1}	activation energy of carbon steel corrosion in Modified McConomy curves, J/mol
F	rotation speed of cylinder, rpm
k	reaction rate constant, $mol^{1-n} \cdot L^{n-1} \cdot s^{-1}$
k_1	reaction rate constant in Modified McConomy curves, $mol^{1-n} \cdot L^{n-1} \cdot s^{-1}$
m_{fc}	mass of fixed carbon, mg
n	corrosion reaction order, dimensionless
r_1	corrosion rate of carbon steel in Modified McConomy curves, $mol^{1-n} \cdot L^{n-1} \cdot s^{-1}$
r_2	coke formation rate on metal surfaces, mg/day
R	gas constant, 8.3145 J/(mol·K)
Re	Reynolds number, dimensionless
t	reaction time, s
T	absolute bulk temperature, K
u_{cyl}	rotation speed of cylinder, m/s

Greek Symbols

μ	dynamic viscosity of oil, Pa·s
ρ	density of oil, kg/m^3
τ_w	wall shear stress, Pa

Subscript

cyl	cylinder
fc	fixed carbon
w	wall

REFERENCES

Albright, L. F., 2008, *Albright's Chemical Engineering Handbook, eds.* Albright, L. F., CRC Press, pp. 1928.

Bota, G. M., 2010, Corrosion of Steel at High Temperature in Naphthenic Acid and Sulfur Containing Crude Oil Fractions, Doctor of Philosophy (PhD), Ohio University.

Coletti, F. and G. F. Hewitt, 4.1.4.1 Thermogravimetric Analysis. *Crude Oil Fouling - Deposit Characterization, Measurements and Modeling*, Coletti, F. and G. F. Hewitt, Elsevier, Vol., pp.

Coletti, F. and G. F. Hewitt, 4.1.5.4 X-ray Diffraction. *Crude Oil Fouling - Deposit Characterization, Measurements and Modeling*, Coletti, F. and G. F. Hewitt, Elsevier, Vol., pp.

Crittenden, B. D., 1988, Chemical Reaction Fouling of Heat Exchangers. *Fouling Science and Technology*, Crittenden, B. D., Netherlands, Kluwer, Dordrecht, Vol., pp. 315-332.

Edwards, L., M. Lubin and J. Marino, 2011, Improving the Repeatability of Coke Bulk Density Testing. *Light Metals 2011*, Edwards, L., M. Lubin and J. Marino, John Wiley & Sons, Inc., Vol., pp. 947-952.

Efird, K. D., E. J. Wright, J. A. Boros and T. G. Hailey, 1993, Correlation of Steel Corrosion in Pipe Flow with Jet Impingement and Rotating Cylinder Tests, *Corrosion*, Vol. 49, pp. 992-1003.

Epstein, N., 1994, A Model of the Initial Chemical Reaction Fouling Rate for Flow within a Heated Tube, and its Verification. *Proc. 10th International Heat Transfer Conference*. G. F. Hewitt. Brighton, UK, Taylor & Francis, Vol., pp. 225-229.

Garverick, L., 1994, *Corrosion in the Petrochemical Industry, eds.* Garverick, L., ASM International, pp.

Groysman, A., 2014, Appendix A.2 Chemical Compounds in Crude Oil and Petroleum Products. *Corrosion in Systems for Storage and Transportation of Petroleum Products and Biofuels: Identification, Monitoring and Solutions*, Groysman, A., Springer Netherlands, Vol., pp. 234.

Javadli, R. and A. de Klerk, 2012, Desulfurization of heavy oil, *Applied Petrochemical Research*, Vol. 1, pp. 3-19.

Javaherdashti, R., C. Nwaoha and H. Tan, 2013, *Corrosion and Materials in the Oil and Gas Industries, eds.* Javaherdashti, R., C. Nwaoha and H. Tan, CRC Press, pp.

Jong, J.-P. d., N.Dowling, M. Sargent, A. Etheridge, A. Saunders-Tack and W. Fort, 2007, Effect of Mercaptans and other organic sulfur species on high temperature corrosion in crude and condensate distillation units. *CORROSION 2007*. Nashville, Tennessee, NACE International, Vol., pp. 1-7.

Joshi, H. M., N. B. Shilpi and A. Agarwal, 2009, Relate Crude Oil Fouling Research to Field Fouling Observations. *International Conference on Heat Exchanger Fouling and Cleaning VIII - 2009*, Schladming, Austria, Vol., pp. 15-16.

Kishore Nadkarni, R. A., 23.4.4 Inductively Coupled Plasma - Mass Spectrometry. *Spectroscopic Analysis of Petroleum Products and Lubricants*, Kishore Nadkarni, R. A., ASTM International, Vol., pp.

Krueger, A. and F. Pouponnot, 2009, Heat Exchanger Performance Enhancement Through the Use of Tube Inserts in Refineries and Chemical Plants - Successful Applications: Spirelf, Turbotal and Fixotal Systems. *International Conference on Heat Exchanger Fouling and Cleaning VIII - 2009*, Schladming, Austria, Vol., pp. 399-406.

Lai, G. Y., 2007, *High-Temperature Corrosion and Materials Applications, eds.* Lai, G. Y., ASM International, pp.

Mrowec, S., T. Walec and T. Werber, 1969, High-Temperature Sulfur Corrosion of Iron-Chromium Alloys, *Oxidation of Metals*, Vol. 1, pp. 93-120.

Mullins, O. C., E. Y. Sheu, A. Hammami and A. G. Marshall, 2007, *Asphaltenes, Heavy Oils, and Petroleomics, eds.* Mullins, O. C., E. Y. Sheu, A. Hammami and A. G. Marshall, Springer New York, pp.

Nikonov, V. A. and A. Senning, 1989, *Sulfur Compounds In Hydrocarbon Pyrolysis, eds.* Nikonov, V. A. and A. Senning, Routledge, pp.

Qu, D. R., Y. G. Zheng, H. M. Jing, Z. M. Yao and W. Ke, 2006, High temperature naphthenic acid corrosion and sulphidic corrosion of Q235 and 5Cr1/2Mo steels in synthetic refining media, *Corrosion Science*, Vol. 48, pp. 1960-1985.

Silverman, D. C., 1984, Rotating Cylinder Electrode for Velocity Sensitivity Testing, *Corrosion*, Vol. 40, pp. 220-226.

Silverman, D. C., 2004, The Rotating Cylinder Electrode for Examining Velocity-Sensitive Corrosion—A Review, *Corrosion*, Vol. 60, pp. 1003-1023.

Slavcheva, E., B. Shone and A. Turnbull, 1999, Review of naphthenic acid corrosion in oil refining, *British Corrosion Journal*, Vol. 34, pp. 125-131.

Stephenson, T., A. Kubis, M. Derakhshesh, M. Hazelton, C. Holt, P. Eaton, B. Newman, A. Hoff, M. Gray and D. Mitlin, 2011, Corrosion-Fouling of 316 Stainless Steel and Pure Iron by Hot Oil, *Energy & Fuels*, Vol. 25, pp. 4540-4551.

Waldo, G. S., R. M. K. Carlson, J. M. Moldowan, K. E. Peters and J. E. Penner-hahn, 1991, Sulfur speciation in heavy petroleums: Information from X-ray absorption near-edge structure, *Geochimica et Cosmochimica Acta*, Vol. 55, pp. 801-814.

Wang, W. and A. P. Watkinson, 2015, Deposition From a Sour Heavy Oil Under Incipient Coking Conditions: Effect of Surface Materials and Temperature, *Heat Transfer Engineering*, Vol. 36, pp. 623-631.

Watkinson, A. P., 2007, Deposition from Crude Oils in Heat Exchangers, *Heat Transfer Engineering*, Vol. 28, pp. 177 - 184.

Watkinson, A. P. and Y.-H. Li, 2009, Fouling Characteristics of a Heavy Vacuum Gas Oil in the Presence of Dissolved Oxygen. *International Conference on Heat Exchanger Fouling and Cleaning VIII - 2009*, Schladming, Austria, Vol., pp. 27-32.

Wiehe, I. A., 2008, 4.3 Phase-Separation Mechanism for Coke Formation. *Process Chemistry of Petroleum Macromolecules*, Wiehe, I. A., CRC Press, Vol., pp. 427.

Wiehe, I. A., 2008, *Process Chemistry of Petroleum Macromolecules, eds.* Wiehe, I. A., CRC Press, pp. 101-119.

Zetlmeisl, M. J., 1996, Naphthenic Acid Corrosion and Its Control. *CORROSION 96*, Denver, Co, NACE International, Vol., pp. 218/211-218/218.